

Seasonal carbon dioxide concentrations and fluxes throughout Denmark's stream network

3 Kenneth Thorø Martinsen¹, Kaj Sand-Jensen^{1*}, Victor Bergmann¹, Tobias Skjærlund¹,
4 Johan Emil Kjær¹, Julian Koch²

⁵ ¹Freshwater Biological Laboratory, Department of Biology, University of Copenhagen,
⁶ Copenhagen, Denmark

⁷ ²Department of Hydrology, Geological Survey of Denmark and Greenland, Copenhagen,
⁸ Denmark

⁹ Corresponding author: Kaj Sand-Jensen (ksandjensen@bio.ku.dk)

10 Key Points:

- Environmental monitoring data and hydrological model outputs can be used to quantify stream CO₂ concentrations and fluxes at national scale
 - Machine learning models can be trained to predict seasonal stream CO₂ concentrations based on catchment and stream characteristics
 - The most important drivers of stream CO₂ are related to landscape morphometry and soil-groundwater-stream connectivity

18 Abstract

19 Streams are important freshwater habitats in large-scale carbon budgets because of their high
20 CO₂ fluxes which are driven by high CO₂ concentrations and surface-water turbulence. High
21 CO₂ concentrations are promoted by terrestrial carbon inputs, groundwater flow, and internal
22 respiration, all of which vary greatly across space and time. We used environmental monitoring
23 data to calculate CO₂ concentrations along with a wide range of predictor variables including
24 outputs from a national hydrological model and trained machine learning models to predict
25 spatially distributed seasonal CO₂ concentrations in Danish streams. We found that streams were
26 supersaturated in dissolved CO₂ (mean = 118 µM) and higher during autumn and winter than
27 during spring and summer. The best model, a Random Forest model, scored R² = 0.46, MAE =
28 46.0 µM, and ρ = 0.72 on a test set. The most important predictor variables were catchment
29 slope, seasonality, height above nearest drainage, and depth to groundwater, highlighting the
30 importance of landscape morphometry and soil-groundwater-stream connectivity. Stream CO₂
31 fluxes determined from the predicted concentrations and gas transfer velocities estimated using
32 empirical relationships averaged 253 mmol m⁻² d⁻¹, and the annual emissions were 513 Gg CO₂
33 from the national stream network (area = 139 km²). Our analysis presents a framework for
34 modeling seasonal CO₂ concentrations and estimating fluxes at a national scale by means of
35 large-scale hydrological model outputs. Future efforts should consider further improving the
36 temporal resolution, direct measurements of fluxes and gas transfer velocities, and seasonal
37 variation in stream surface area.

38 Plain Language Summary

39 Streams play an essential role in the global carbon cycle as they usually are very rich in CO₂ and
40 thus emit much CO₂ to the atmosphere To estimate how much CO₂ is emitted from streams, we
41 used environmental data to calculate CO₂ concentrations and a wide range of terrain and stream
42 flow characteristics. We used this data to train a machine learning model to predict seasonal
43 stream CO₂ concentrations across Denmark. We found that CO₂ concentrations in Danish
44 streams were generally higher during autumn and winter than during spring and summer. The
45 key factors determining CO₂ concentrations included terrain slope, seasonality, elevation relative
46 to nearby streams, and depth to groundwater. From the national stream CO₂ concentrations, we
47 estimated the exchange of CO₂ between stream and atmosphere and the annual emissions. This
48 study demonstrates how machine learning models and data from multiple sources can be used to
49 predict stream CO₂ concentrations at large scales. The framework and model allow us to quantify
50 and manage the CO₂ emissions from streams at a national scale.

51 1 Introduction

52 Freshwater ecosystems, particularly running waters such as rivers and streams (the term
53 streams used from here), play a crucial role in the global carbon cycle (Raymond et al., 2013).
54 They link terrestrial habitats to the sea, and facilitate the transport and processing of carbon
55 (Cole et al., 2007). Mineralization of organic matter within streams produces carbon dioxide
56 (CO₂), which, along with substantial external sources, contributes to the commonly observed
57 supersaturation of dissolved CO₂ (Hotchkiss et al., 2015). This makes streams open windows of
58 CO₂ emission to the atmosphere (Butman et al., 2016; Wallin et al., 2013). Spatiotemporal CO₂
59 dynamics comprise a complex interplay of biotic and abiotic factors.

The extensive variability of CO₂ concentrations in streams are well documented (Marx et al., 2017; Sand-Jensen et al., 2022a). This variability is primarily driven by the dynamic nature of groundwater and terrestrial contributions (Duvert et al., 2018; Humborg et al., 2010), and by the hydrology and biological processes that influence both the flow of water and organic matter in streams and the gas flux across the air-water interface (Hutchins et al., 2019; Long et al., 2015). These processes are subject to seasonal variations which can be attributed to direct climatic drivers, such as temperature and runoff fluctuations, or indirect effects mediated by local riparian or catchment-scale factors, like terrestrial vegetation cover and land use changes. Consequently, incorporating seasonality is crucial for enhancing the predictive capabilities of current models for CO₂ concentrations in streams. Current methods to predict spatiotemporal stream CO₂ concentrations are limited and the temporal component is often neglected (Lauerwald et al., 2015; Martinsen et al., 2020) or only cover one or few catchments. One recent exemption is Liu et al. (2022), who predicted monthly CO₂ concentrations in streams at a global scale. To address this gap, our study combines traditional spatial data with hydrological model outputs to improve seasonal predictions of stream CO₂ concentration.

Hydrology influences stream CO₂ concentrations. In particular, water velocity and discharge influence CO₂ concentrations directly, because they drive water turbulence and gas transfer velocity and thus CO₂ exchange with the atmosphere. Furthermore, discharge also influences lateral inputs of organic matter and dissolved CO₂ from land (Liu & Raymond, 2018). Groundwater is generally CO₂ supersaturated and contributions are constrained by local hydrogeological and topographical settings (Crawford et al., 2014; Duvert et al., 2018). Partitioning discharge into the constituting flow components could potentially improve predictions of CO₂ concentrations because different flow components are expected to have different CO₂ concentrations (Sand-Jensen et al., 2022a). Detailed hydrological models that integrate groundwater and surface water processes are required for quantifying flow contributions in space and time. By combining traditional spatial data with hydrological model outputs, we aim to provide more robust and process-constrained seasonal predictions of stream CO₂ concentrations and gas transfer velocities, ultimately enabling better estimates of spatiotemporally upscaled CO₂ fluxes.

Machine learning algorithms offer a promising approach to predicting CO₂ concentrations in streams (Martinsen et al., 2020). By leveraging large datasets of monitoring data and relevant predictor variables, machine learning models can learn patterns and relationships that are not easily identifiable through traditional statistical methods (Breiman, 2001). The advantages include improved accuracy and flexibility in modeling nonlinear relationships, as well as their interactions (Olden et al., 2008). However, model interpretation can be challenging due to the complexity of the algorithms (James et al., 2013). Traditional approaches rely heavily on simplifying assumptions and parameterizations, whereas machine learning models are less transparent in their calculations. Ultimately, integrating machine learning with the outputs of traditional modeling frameworks could lead to more accurate and robust predictions of stream CO₂ concentrations, offering insights into the complex processes governing carbon cycling in freshwater ecosystems and permitting upscaling of fluxes to regional and national scales.

In this study, we compile country-level data consisting of static catchment characteristics and dynamic hydrological variables derived from a national hydrological model. With this data, we apply machine learning methods to predict seasonal CO₂ concentrations throughout the

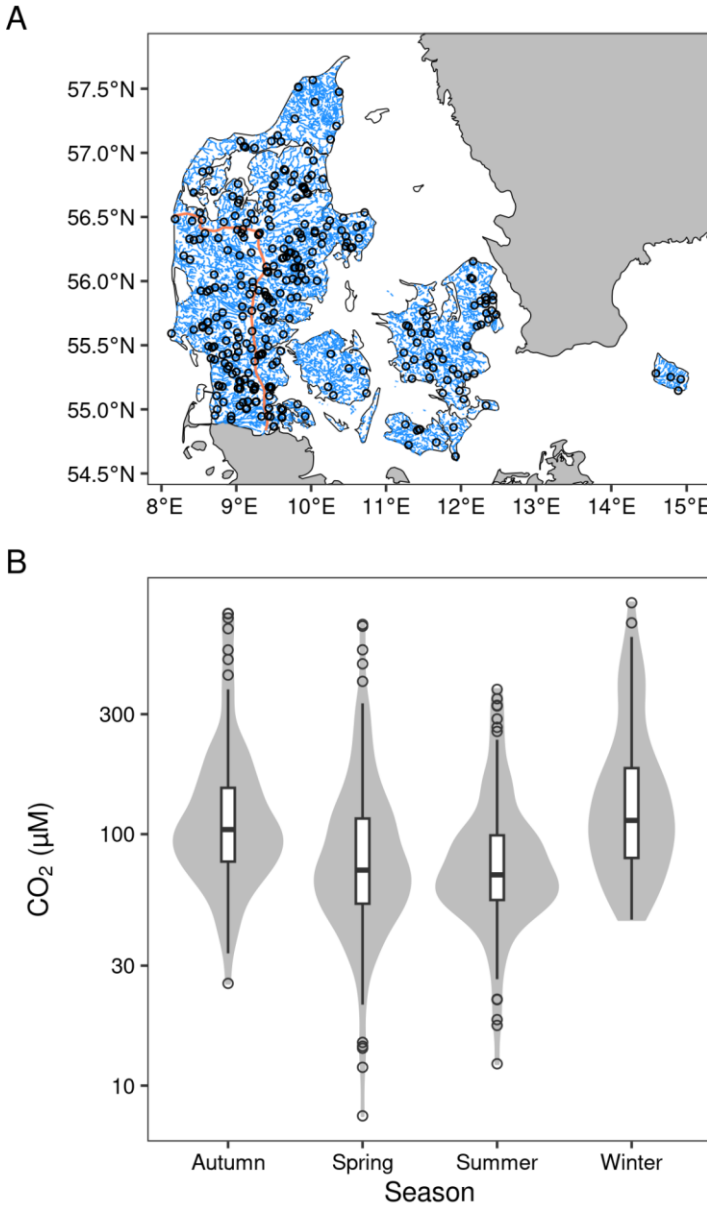
105 Danish stream network. We hypothesize that: 1) seasonality is an important predictor of CO₂
106 concentrations in streams, and 2) hydrological flow components, in particular groundwater
107 inflow, influence both CO₂ delivery and emissions and should therefore improve predictability of
108 CO₂ concentrations in streams. We use the predicted CO₂ concentrations and hydrological data
109 to estimate CO₂ fluxes and compare these with *in-situ* measurements. Finally, we upscale CO₂
110 fluxes from the entire Danish stream network.

111 **2 Materials and Methods**

112 We employed a model selection approach to identify the optimal model for predicting
113 seasonal CO₂ concentrations. CO₂ concentrations were derived from observations of pH and
114 alkalinity obtained through the national environmental monitoring program. Additionally, a suite
115 of hydrological and landscape environmental variables, expected to influence stream CO₂
116 dynamics, were included as predictor variables (Table S1). CO₂ observations were aligned with
117 the locations along the stream network where the national hydrological model of Denmark (DK-
118 Model), simulates discharge and flow components. For both the monitoring and DK-Model
119 outputs, we used data spanning a range of 10 years from 2000 to 2009. The predicted CO₂
120 concentrations were used to estimate the CO₂ flux using the hydrological model components and
121 aggregated to obtain national CO₂ emission estimates. The estimated seasonal CO₂ fluxes are
122 compared to *in-situ* measurements.

123 2.1 Study region

124 The topography of Denmark is generally low-relief with elevations above sea-level
125 ranging from -18 to 172 m, mean annual precipitation of 2.3 mm d⁻¹, and mean air temperature
126 of 9.0 °C, during the study period. The majority of soils are calcareous in nutrient-rich moraine
127 landscapes, except for SW-Jutland which was not covered during the Weichselian glaciation and
128 has mainly well-leached, sandy soils lower in carbonate and clay minerals (Figure 1 A). Due to
129 mineral weathering, this has resulted in differences in water chemistry between the less alkaline
130 SW-Jutland and more alkaline major parts of Denmark. The land use is dominated by agriculture
131 (approx. 60 %).



132

133 **Figure 1.** A) Map showing the stream network included in the DK-model (blue) and stream sites
 134 (open points) with one or more observations of seasonal CO₂ concentration. The orange line
 135 represents the maximum extent of the ice sheet during the most recent ice age where eastern
 136 Denmark was covered by ice and SW-Jutland remained ice-free. B) Density distributions (grey)
 137 and boxplots of seasonal CO₂ concentrations. Box plots show median (solid horizontal line),
 138 25% and 75% quartiles (upper and lower hinge), lines extending to one and a half times the inter-
 139 quartile range (upper and lower whisker), and observations outside this range (points).

140

141 2.2 Predicting stream CO₂ concentrations142 2.2.1 CO₂ concentrations

143 Stream CO₂ concentrations were calculated from daytime measurements of alkalinity,
144 pH, and water temperature sampled as part of the national environmental monitoring program
145 (Lauridsen et al., 2005). Specifically, we calculated CO₂ concentrations using the AquaEnv R-
146 package (Hofmann et al., 2010). Estimates of CO₂ from alkalinity and pH are subject to high
147 uncertainty in low-alkalinity (< 1 meq L⁻¹), acidic, often humic waters, with an increasing degree
148 of overestimation as alkalinity decreases further towards zero (Abril et al., 2015). However,
149 Danish catchments are generally rich in carbonate minerals resulting in alkaline waters, and
150 show close agreement between measured CO₂ concentrations and those estimated from alkalinity
151 and pH (Sand-Jensen et al., 2022a). In our data, 21.6% of observations were below 1 meq L⁻¹ and
152 4% below 0.5 meq L⁻¹. To avoid unrealistically high values, we excluded observations with low
153 pH (<5.4; 0.6% of observations) and very high estimated CO₂ concentrations (40,000 μatm;
154 0.05% of observations) similar to other studies (Hastie et al., 2018; Martinsen et al., 2020). We
155 determined seasonal means for sites with 4 or more observations resulting in 745 seasonal CO₂
156 concentrations from 309 sites for further analysis.

157 2.2.2 Catchment delineation

158 We delineated the topographical catchment areas for each of the 62,726 DK-Model
159 surface water simulation points (Q-points) using a digital elevation model (DEM) with a
160 resolution of 10 m, resampled from a high-resolution (1.6 m) national DEM (SDFI, 2021). DEM
161 processing and catchment delineation were carried out using the WhiteboxTools and TauDEM
162 software (Lindsay, 2016; Tarboton, 2017). Specifically, the DEM was preprocessed to remove
163 hydrological sinks, areas where water would accumulate due to cells being surrounded by higher
164 elevations, using a hybrid breaching and filling approach (Lindsay, 2016). This was followed by
165 determination of flow directions using the deterministic-eight flow scheme (O'Callaghan &
166 Mark, 1984). We extracted a virtual stream network and snapped DK-model Q-points to this
167 network with a maximum distance of 100 m and delineated the catchment area.

168 2.2.3 Dynamic hydrological and meteorological variables

169 We included hydrological and meteorological variables for each stream site and season.
170 Simulated discharge and four flow components from the DK-Model were used for further
171 analysis. The DK-Model is a physically based and spatially distributed hydrological model that,
172 using the MIKE SHE model code, integrates groundwater, surface water, and anthropogenic
173 activities. The DK-Model has been developed by the Geological Survey of Denmark and
174 Greenland over the last 25 years (Henriksen et al., 2023; Højberg et al., 2013; Soltani et al.,
175 2021) and is currently used in basic research and a range of applications such as national water
176 resources assessments, status of water resources, and adaptation to climate change. The DK-
177 model simulates daily flow components and total discharge at 62,726 Q-points throughout the
178 stream network. The flow components are simulated locally and are added to the total discharge
179 which aggregates all upstream flow contributions. The components are 1) overland inflow (OF),
180 2) groundwater inflow (GWF), 3) drainage inflow from groundwater (DF), and 4) and drainage
181 inflow from ponded water (DPF) (Figure S1). OF represents water flow on the terrain following
182 topographical gradients and the process is initiated in a grid cell when the overland storage
183 exceeds predefined detention storage. GWF represents the direct exchange between groundwater

184 and surface water. Most streams in Denmark are associated with a positive GWF, indicating that
185 groundwater contributes as baseflow to the discharge generation. Such a condition is referred to
186 as gaining streams and initiated by an upward groundwater gradient in the stream channel. DF
187 represents water that moves from groundwater storage to local surface waters and DF is initiated
188 in a grid cell when the groundwater level exceeds a predefined drain depth. Within the DK-
189 model, DF is expected to represent tile drainage from agricultural fields. Since detailed data on
190 the location and effectiveness of tile drains are absent at national scale, the drain flow process
191 representation is calibrated against streamflow observations to obtain effective parameter values.
192 DPF represents processes of urban drainage networks and ponded water that moves to local
193 surface waters. Typically, DF constitutes a major part of the generated flow and is highly
194 variable in time with the largest flows occurring during winter and spring when groundwater
195 levels are highest. GWF varies less in time than DF and contributes much of the flow generated
196 during summer. OF and DPF are more variable in time and space and are driven by intense
197 precipitation events.

198 We removed Q-points that were located within lakes (3172), specific to the DK-model
199 (2741), more than 100 meters away from the virtual stream network (3810), and/or did not
200 intersect the digital elevation model (613). For each DK-model Q-point, daily discharge and the
201 four flow components were averaged seasonally. From national climate grids, we extracted
202 seasonal mean precipitation (10 km grid) and air temperature (20 km grid) for each catchment
203 (Scharling, 1999a, 1999b).

204 2.2.4 Static variables

205 The static attributes are stated in three different ways: 1) as average values of relevant
206 map layers over the catchment area, 2) as site-specific values, or 3) as locally aggregated
207 statistics using a 200 m buffer analysis. These map layers included for example slope and
208 hydrological landscape indices such as height above the nearest drainage (HAND), derived from
209 the 10 m DEM. HAND represents the vertical distance between a terrain grid cell and the stream
210 grid cell it drains to (Rennó et al., 2008). We extracted land use from a national 10 m dataset
211 (Levin, 2022), geology-related variables (Adhikari et al., 2013), and the simulated groundwater
212 depth averaged over time of the DK-Model. Furthermore, we identified land use in the near
213 upstream area using the intersection between a circular 200 m buffer zone and the catchment for
214 each site. See Table S1 for a detailed overview of the predictor variables.

215 2.2.5 Modeling

216 We split the data into a training (80%) and test (20%) dataset. We grouped observations
217 by stream site such that observations from the same site were not split during resampling. Inter-
218 correlation between numeric predictor variables was assessed using Pearson correlation. Before
219 modeling, the ‘season’ predictor variable was one-hot encoded, and numeric predictor variables
220 were preprocessed by applying the Yeo-Johnson power transformation followed by zero-mean
221 and unit variance standardization. Using the training data, we explored the performance of
222 several different models by 5-fold cross-validation (outer loop) to select the best model. Many
223 machine learning models require tuning of hyperparameters for optimal performance. We
224 defined hyperparameter search spaces which were sampled using 50 iterations of random search
225 and evaluated using 5-fold cross-validation (inner loop). Model selection was performed using
226 nested cross-validation. The best model was then trained on the entire training dataset, evaluated

on the test set, and used to make predictions for all DK-model sites (53668). To assess model performance, we determine the R^2 , root mean squared error (RMSE), mean absolute error (MAE), Pearson correlation coefficient (ρ), and mean absolute percentage error (MAPE). The influence of predictor variables on CO₂ concentrations in the best model was investigated using permutation variable importance and partial dependence plots. To explore the influence of the number of training observations on model performance we assessed cross-validated performance using random subsets of the training data of different sizes. Machine learning models were trained and evaluated using the Python scikit-learn library (Pedregosa et al., 2011).

235 2.3 Estimating stream CO₂ fluxes

2.3.1 CO₂ flux estimates

237 The CO₂ flux is the product of the gas transfer velocity (k) and the air-water
 238 concentration gradient:

$$F = k(CO_{2-water} - CO_{2-sat}) \quad \text{Eq. 1}$$

We estimated CO₂ flux from the predicted seasonal CO₂ concentrations and empirical relationships for k assuming an atmospheric partial pressure of 400 μatm for the study period 2000–2009. Partial pressure was converted to concentration using Henry's Law as a function of water temperature. Seasonal water temperature was estimated for all sites using a fitted linear relationship between observed water temperatures and air temperatures (Figure S2). k_{600} (m d⁻¹), k normalized to a Schmidt number of 600 (CO₂ at 20 °C), was estimated as a function of water velocity (v, m s⁻¹) and slope (s, dimensionless) based on the relationship ($k_{600} = v \times s \times 2841 + 2.02$) from Raymond et al. (2012). k at the ambient temperature is determined using the ratio of Schmidt numbers based on relationships in Jähne et al. (1987) and Wanninkhof (1992). Water velocity was estimated from DK-model derived discharge (m³ s⁻¹) using hydraulic geometrical relationships ($v = 0.19 \times Q^{0.29}$; Raymond et al., 2012), and the slope was determined for each stream segment of the virtual stream network using TauDEM. CO₂ fluxes could be estimated for 53.653 DK-model q-points.

2.3.2 CO₂ flux measurements

To validate the estimated CO₂ fluxes we measured daytime CO₂ fluxes using floating chambers multiple times across Denmark (Rivers Tryggevælde, Odense, Omme, and Tude) resulting in 54 measurements from 27 stream sites. Floating chambers were equipped with small, inexpensive sensors (SenseAir, Sweden) as described in Bastviken et al. (2015) measuring the headspace CO₂ partial pressure every 30 or 60 seconds for at least 20 minutes. The flux was determined by the change in CO₂ partial pressure over time:

$$F = \frac{dCO_2}{dt} \frac{VP}{RTA} \quad \text{Eq. 2}$$

Where dCO_2/dt is the slope estimate by linear regressions, P is the atmospheric pressure (atm), V is the chamber volume (0.008 m^3), A is the chamber area (0.075 m^2), R is the gas constant ($\text{m}^3\text{ atm K}^{-1}\text{ mol}^{-1}$) and T is the temperature (Kelvin). We used the average flux determined from two or three chambers at each visit. On most occasions, we measured pH in the field (YSI Professional Plus, USA) and collected water samples for measuring alkalinity using Gran titration (Gran, 1952) and to calculate the CO_2 concentration. We also determined k from

267 the observed CO₂ concentration and flux according to eq. 1, and normalized k to k₆₀₀ for
268 comparisons.

269 2.3.3 Upscaling CO₂ fluxes

270 We determined the annual CO₂ flux from the Danish stream network using the estimated
271 fluxes. We sampled the stream network at 100 m resolution (191.165 sites), estimated stream
272 width for all sites, and used nearest neighbor interpolation to determine the flux. Stream width
273 was determined as a function of catchment area using empirical relationships in Denmark for six
274 geographical regions (Table S2; Olsen & Højberg, 2011). Based on this analysis, the average
275 stream width was 7.3 m with a standard deviation of 6.5 m. Since the relationships were based on
276 the catchment area, the stream area did not differ between seasons. Finally, the annual flux was
277 determined by multiplying the flux, stream width, and resolution used for sampling the stream
278 network before aggregating by season. The upscaling procedure proved insensitive to the applied
279 sampling resolution.

280 **3 Results**

281 3.1 CO₂ concentrations

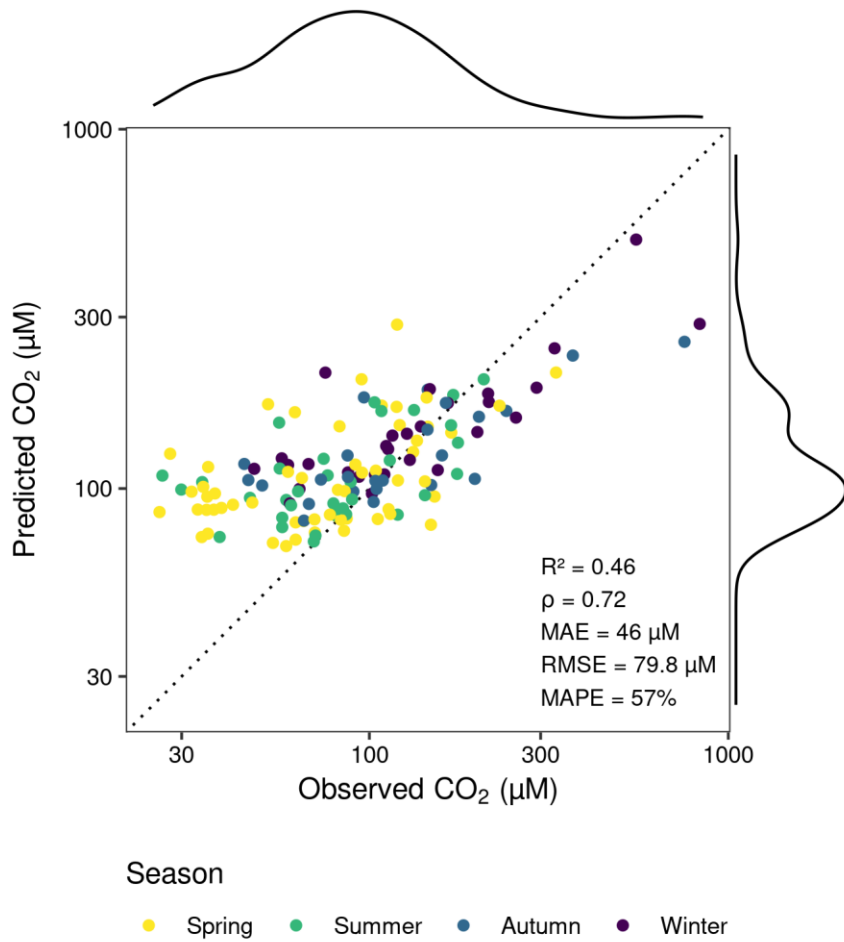
282 For the 745 seasonal observations used in the analysis, the mean alkalinity was 2.6 (range
283 0.05–7.6) meq L⁻¹ with a pH of 7.7 (range 6.0–8.7). The mean CO₂ concentration was 118 (range
284 8–832) μM with significant seasonal differences (One-way ANOVA, F = 21.2, p-value <
285 0.0001). Concentrations were lower in spring and summer compared to autumn and winter but
286 there were no pairwise differences between winter vs autumn or spring vs summer (Figure 1 B).
287 737 observations (98.9 %) had CO₂ concentrations above air saturation, highlighting the
288 prevalence of CO₂ supersaturation in streams.

289 3.2 Modeling CO₂ concentrations

290 We evaluated the performance of several models for predicting seasonal stream CO₂
291 concentrations from catchment characteristics, hydrology, and climate (Table S3). Many of the
292 models performed poorly indicating that relationships between CO₂ concentrations and predictor
293 variables were complex. Furthermore, the performance of the 5 cross-validation folds was
294 subject to high variability. Based on all performance metrics, the Random Forest model showed
295 superior performance and was therefore selected for further analysis. Following training on the
296 entire training data, the Random Forest model was evaluated on the test set ($R^2 = 0.46$, MAE =
297 46.0 μM, RMSE = 79.8 μM, ρ = 0.72, and MAPE = 57 %). The model appeared to over-predict
298 at lower CO₂ concentrations which was most common in spring and summer (Figure 2).

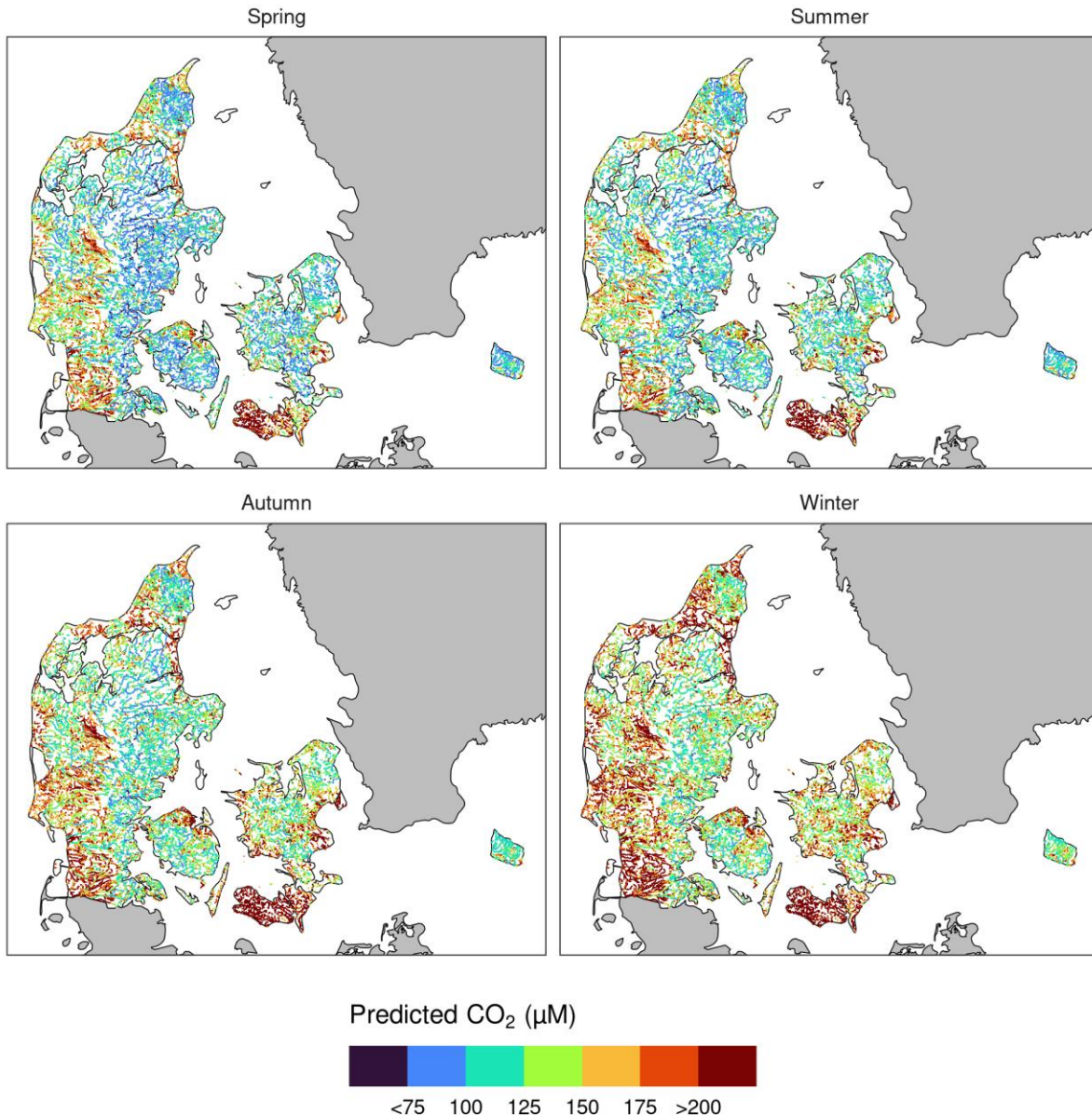
299 The model was used to make seasonal predictions for all DK-model Q-points (Figure 3).
300 At the regional scale, predicted CO₂ concentrations were related to geology with high
301 concentrations in the glacial outwash plains west of the main stationary line of the most recent
302 ice age, i.e. SW-Jutland (Figure 1 A) and in the southern islands with low relief landscape. The
303 performance estimated during model selection (Table S3) and the performance determined on the
304 test set were quite different. We investigated the sensitivity of the model to different sizes of
305 training data and found that performance increased with the size of the training data and
306 variability between cross-validation folds remained substantial (Figure S3).

307



308

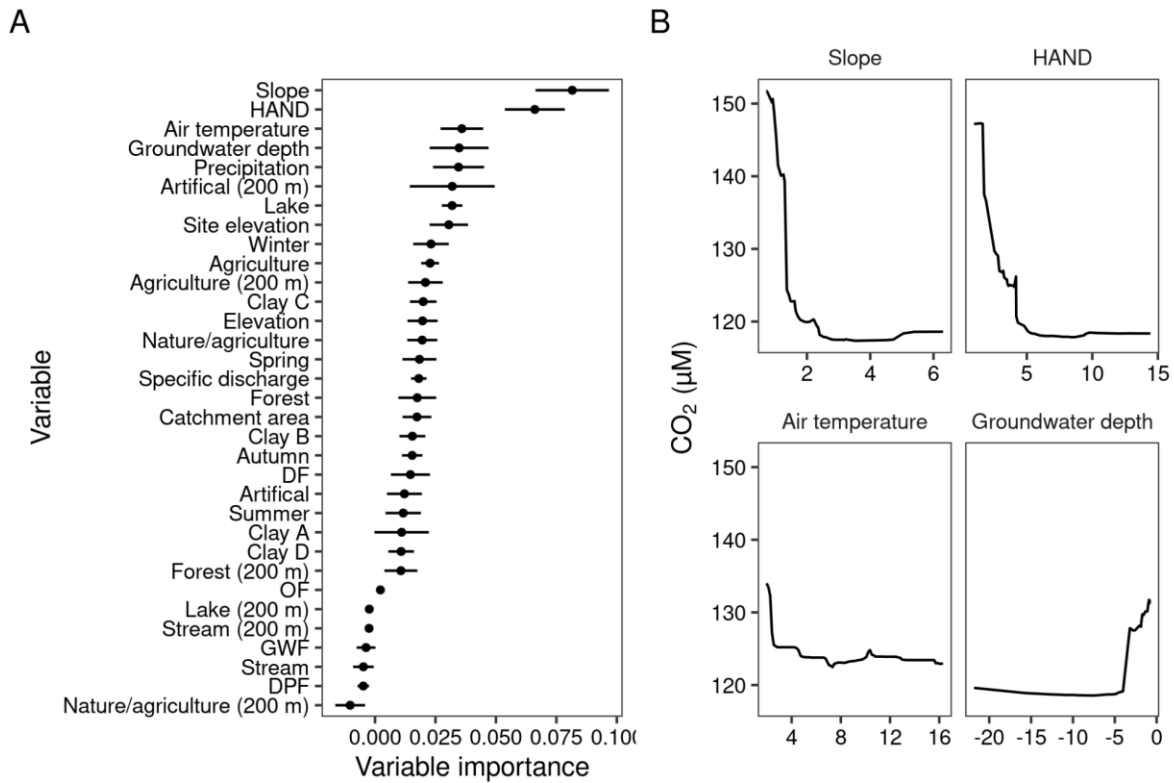
309 **Figure 2.** Observed (x-axis) and predicted values (y-axis) of stream CO_2 concentrations (μM)
310 from the test set colored by season with density distributions on the margins. Predicted CO_2
311 concentrations are based on a Random Forest model.



312 **Figure 3.** Predictions of CO_2 concentration for each season (A-D) covering Denmark based on a
 313 Random Forest model. The stream network consists of sites included in the hydrological DK-
 314 model.

315 We explored the importance of the predictor variables and their relationship to stream
 316 CO_2 concentrations. The most important predictor was the mean catchment slope, followed by
 317 height above nearest drainage (HAND), and air temperature (Figure 4 A). The functional
 318 relationships, without considering interactions, were generally as expected (Figure 4 B). The
 319 influence of slope and HAND was most pronounced at low mean catchment slopes and HAND,
 320 indicating that CO_2 concentrations are higher in streams in flat terrain where contact between
 321 stream water and soils is likely to be high. The response to temperature followed the expectation

322 that CO₂ concentrations would be greater during winter and lower in summer. Several of the
 323 predictor variables, e.g., catchment slope, were related to other predictor variables (Figure S4).



324

325 **Figure 4.** A) Mean (point) \pm standard deviation (line range) permutation variable importance
 326 computed on the test set for all predictor variables. B) Relationship between predicted CO₂
 327 concentration (y-axis) and the four most important predictor variables (x-axis) determined using
 328 partial-dependence plots.

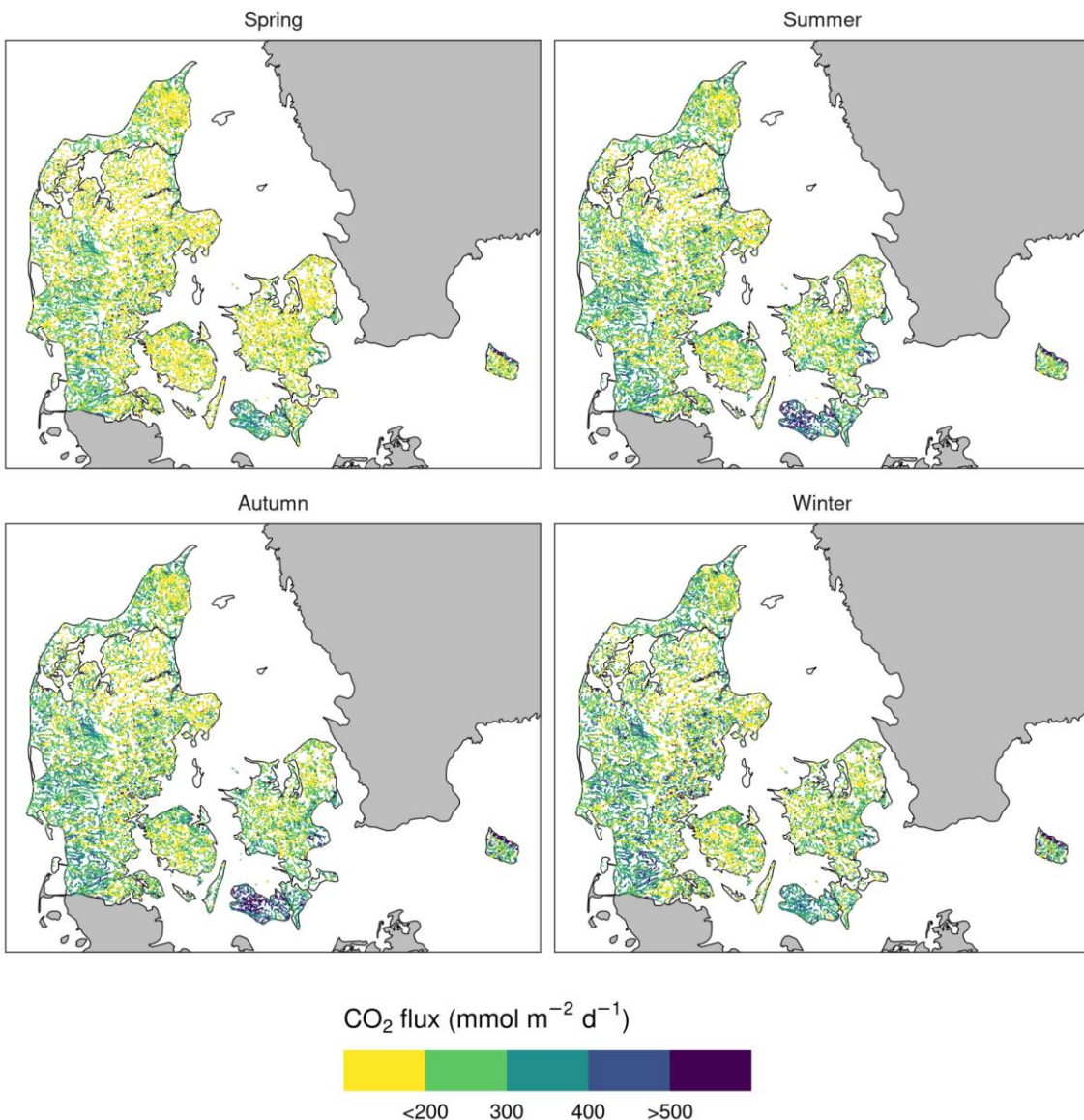
329 3.3 CO₂ fluxes

330 CO₂ fluxes determined from the predicted CO₂ concentration and estimated k had an
 331 overall mean of 253 mmol m⁻² d⁻¹ with the highest fluxes during winter and lowest during spring
 332 (Table 1). We estimated the CO₂ flux for all sites to produce national maps of seasonal CO₂
 333 fluxes (Figure 5). The maps highlight regions with high CO₂ fluxes, e.g. SW-Jutland and
 334 Lolland-Falster, which coincide with areas with high predicted CO₂ concentrations (Figure 3).
 335 Spatial patterns of CO₂ flux within the stream network were consistent with expectations. Lower
 336 CO₂ concentrations were observed at lake outlets during summer and increased gradually with
 337 increasing distance downstream from the outlets (Figure 6).

Season	Q _{2.5%}	Q _{50%}	Q _{97.5%}	Mean
Autumn	118	237	593	268
Spring	89	191	492	218
Summer	115	225	529	253
Winter	118	241	651	276

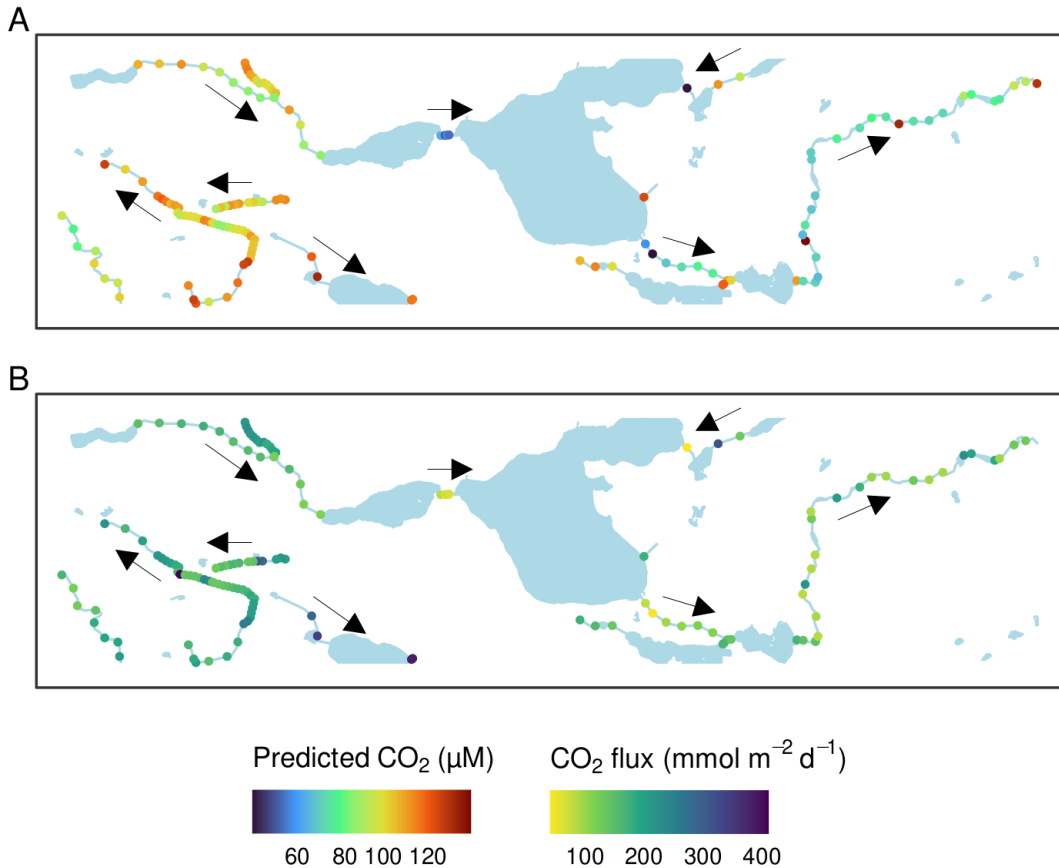
338 **Table 1.** Summary statistics of estimated stream CO₂ fluxes (mmol m⁻² d⁻¹) for each season. The
339 fluxes were estimated from predicted CO₂ concentrations and empirical hydrological
340 relationships.

341



342

343 **Figure 5.** Estimated CO₂ flux for each season (A-D) covering Denmark. The fluxes are
344 estimated from predicted CO₂ concentrations and empirical hydrological relationships. The
345 stream network consists of sites included in the hydrological DK-model.
346

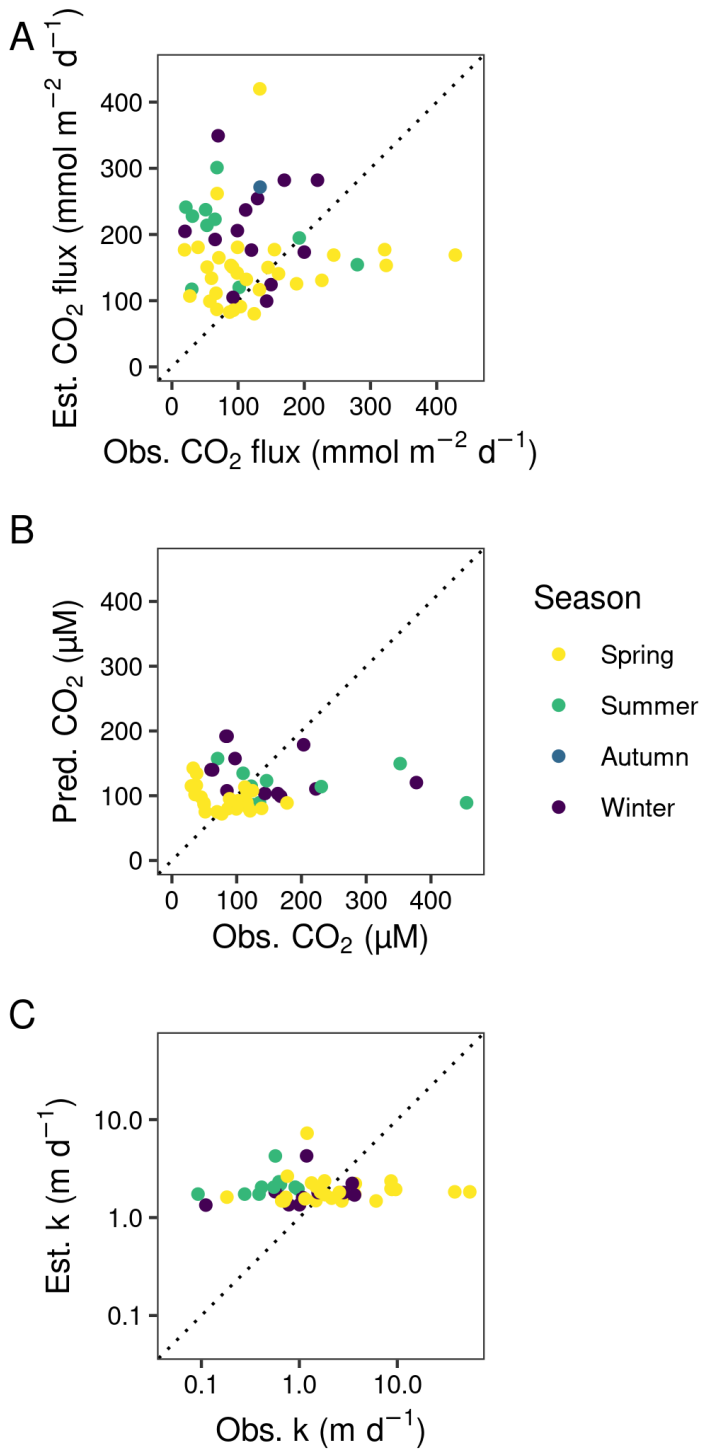


347 **Figure 6.** Predicted CO_2 concentration (A) and estimated fluxes (B) during summer around Lake
 348 Fure, north of Copenhagen. The geographical area is approximately 5 by 20 km with the stream
 349 network and lakes larger than 10^4 m^2 shown in blue. Three sites with high estimated CO_2 flux
 350 have been removed to improve visualization.

351 Floating chamber measurements of CO_2 fluxes had a mean of $186 \text{ mmol m}^{-2} \text{ d}^{-1}$ and a
 352 larger variation than the estimated flux (range 80 – $349 \text{ mmol m}^{-2} \text{ d}^{-1}$). We found good agreement
 353 between observed and estimated CO_2 fluxes for some of the observations, while others had been
 354 substantially overestimated (Figure 7 A). Observed and estimated CO_2 concentrations showed
 355 better agreement than the corresponding k -values.

356

357



358

359 **Figure 7.** Estimated and observed stream CO₂ flux (A), CO₂ concentration (B), and k (C)
 360 colored by season and the 1:1 relationship (dotted line). Observed CO₂ concentrations were
 361 determined from pH and alkalinity, estimated k based on empirical relationships, and estimated
 362 CO₂ flux from estimated k and CO₂ concentration predicted by a Random Forest model.

363 Based on the national stream CO₂ flux estimates we calculate aggregated national
 364 estimates of 512.6 Gg CO₂ year⁻¹ (spring = 440.3, summer = 513.4, autumn = 541.2, and winter
 365 = 555.2 Gg CO₂ year⁻¹). The total stream area was 139 km² yielding an annual average of 3675 g
 366 CO₂ m⁻² stream y⁻¹ or 11.9 g CO₂ m⁻² y⁻¹ for Denmark's total surface area (43,100 km²).

367 4 Discussion

368 4.1 Predicting stream CO₂ concentrations

369 We show how a machine learning approach can be used to predict stream CO₂
 370 concentrations from catchment features, similar to other studies (Lauerwald et al., 2015;
 371 Martinsen et al., 2020) and expand with two key aspects, namely adding seasonal resolution and
 372 including dynamic hydrological features from a national scale hydrological model. The predicted
 373 CO₂ concentrations in Danish streams are as expected generally supersaturated (Rebsdorf et al.,
 374 1991) and lowest in spring and summer and higher during autumn and winter (Jones &
 375 Mulholland, 1998; Sand-Jensen & Staehr, 2012). This influence of seasonality was evident from
 376 the response to air temperature with highest CO₂ concentrations in winter at low surface
 377 irradiance and photosynthetic activity and thus not a direct effect of air temperature. Visual
 378 assessment of the map of predicted CO₂ concentrations revealed localized deviations from the
 379 expected pattern observed in adjacent sites. These discrepancies likely originated from errors in
 380 the catchment delineation, resulting in disparate predictions for seemingly similar stream sites.
 381 Employing a higher resolution DEM could have potentially mitigated these discrepancies and
 382 improved predictions in these specific areas. Within the stream network, summer CO₂
 383 concentrations at lake outlets were substantially reduced, approaching the atmospheric
 384 saturation, due to higher residence time with air contact and primary production in lakes (Sand-
 385 Jensen et al., 2022a; Weyhenmeyer et al., 2012). The lake effect is pronounced downstream of
 386 the common eutrophic lakes in Denmark, where dissolved CO₂ essentially is consumed entirely,
 387 while the concentration increases with distance downstream from the lake outlet (Sand-Jensen et
 388 al., 2022a). Seasonal resolution of CO₂ concentrations is not only important for improving the
 389 accuracy of stream CO₂ fluxes but also for modeling performance and distribution of aquatic
 390 macrophytes whose rates of photosynthesis depend on CO₂ concentrations (Demars &
 391 Trémolières, 2009; Sand-Jensen et al., 2022b).

392 Surprisingly, the hydrological variables were not among the most important predictors.
 393 We expected that DF would be important, as this flow component is expected to be very rich in
 394 dissolved CO₂ originating from soil respiration (Halbedel & Koschorreck, 2013; Marx et al.,
 395 2017; Sand-Jensen & Staehr, 2012). However, DF and OF components are more event-driven, in
 396 contrast to GWF which is more constant over time. The event-driven contributions may be
 397 neglected at the seasonal timescale applied in the analysis. Moreover, the flow components
 398 represent contributions resulting from processes simulated for a discrete location, which is very
 399 sensitive to the parameterization of the underlying hydrological model around that location, i.e.
 400 conceptualization of hydrogeological layers or drain flow. Other predictors such as mean
 401 groundwater depth and HAND, which are also expected to be correlated with water table depth

(Koch et al., 2021; Rennó et al., 2008), are however important variables. Rocher-Ros et al. (2019) also found that a depth-to-water index improved predictions of stream CO₂ concentrations, highlighting the importance of soil-groundwater-stream interactions which can be highly discrete (Duvert et al., 2018; Lupon et al., 2019), calling for increased spatial sampling resolution. Similarly, catchment slope emerges as the most important predictor in agreement with several other studies (Lauerwald et al., 2015; Liu et al., 2022; Martinsen et al., 2020). Catchment slope may affect stream CO₂ concentrations in several ways but most importantly influences catchment carbon accumulation, i.e. longer storage in low-slope landscapes, and higher CO₂ flux across the air-water interface (Smits et al., 2017; Wallin et al., 2011) indicating why slope repeatedly emerges as an essential proxy of stream CO₂ concentration.

412 4.2 Estimating and measuring stream CO₂ fluxes

The relationship between estimated and *in-situ* CO₂ fluxes is poor. While the spatial and temporal coverage of the *in-situ* measurements is not high, they provide an initial evaluation of the estimated CO₂ fluxes which is often lacking in large-scale studies. While we did expect a better relationship, there is an apparent scale issue when comparing instantaneous and seasonal fluxes. The discrepancies appear to be larger during summer and similarly for test set predictions of CO₂ concentrations where the overestimated values are predominantly observations during spring. Spring and summer are seasons where ecosystem metabolism is highest (Kelly et al., 1983; Sand-Jensen & Frost-Christensen, 1998), and expectedly also the within-site variation. Consequently, diel variations in CO₂ concentrations can be pronounced (Sand-Jensen et al., 2022a) complicating the comparison between instantaneous measurement and seasonally predicted CO₂ concentrations. Accounting for the type of primary producers, e.g. benthic algae or submerged macrophytes, could improve future modeling efforts as reaches dominated by the latter appear to have prolonged periods of high production in contrast to that of benthic algae which are more temporally variable (Alnooe et al., 2016, 2020).

In the comparison of estimated and *in-situ* CO₂ fluxes, the overestimated fluxes appear to be a result of overestimated k values while CO₂ concentrations showed better agreement. Many of the overestimated fluxes were from the same sites, e.g., six observations are from two sites close to each other in River Tryggevælde and three are from the same site in River Odense. This suggests that the estimated fluxes are not suitable for local (stream site) considerations but rather regional estimates of stream CO₂ fluxes. k is estimated in two steps using discharge and slope (Raymond et al., 2012) where the latter is more reliably determined from elevation models. However, the estimation of velocity solely based on discharge appears to introduce much higher uncertainty (Liu et al., 2022) which is also evident from the empirical relationship explaining a relatively low proportion of the variation ($R^2 = 0.49$). While aggregating multiple observations or empirical relationships may reduce the variability, there is a need for improved relationships to predict k in large-scale studies. Furthermore, the empirical relationship for k has a rather high intercept (2.02 m d⁻¹; Raymond et al., 2012). Lower k values have been reported in the literature (Sand-Jensen & Staehr, 2012; Wallin et al., 2011), suggesting a potential bias in upscaling, particularly in lowland regions like Denmark. Better knowledge of stream cross-sections or using hydrodynamic models that directly simulate velocity would likely improve estimates but might be difficult or computationally expensive to apply at scale. There has been recent progress in the development of empirical relationships, e.g., Ulseth et al. (2019) identified different relationships for k in low- and high-energy streams but other variables might also cause differences in k or water velocity for otherwise similar streams including wind-exposure (Beaulieu et al., 2012),

447 surface-films (Salter et al., 2011), and high submerged macrophyte biomass that markedly
448 reduce mean velocity and introduce extensive small-scale variability of velocity within and
449 outside macrophyte patches (Sand-Jensen, 2008; Sand-Jensen & Mebus, 1996). Developing
450 relationships for k and differentiating between streams based on the most important drivers of k
451 could further improve the models (Thyssen & Erlandsen, 1987; Wang et al., 2021), which is
452 particularly important for small, lowland stream networks where CO₂ concentrations are high.

453 4.3 Large-scale CO₂ flux estimates

454 The estimated average national stream CO₂ flux (3675 g CO₂ m⁻² stream y⁻¹) was of
455 similar magnitude to those found in other studies when normalized by stream area. For Sweden,
456 Hamburg et al. (2010) estimated 6785 g CO₂ m⁻² y⁻¹ and Wallin et al. (2018) estimated 14,104 g
457 CO₂ m⁻² y⁻¹ only for low-order (1–4) streams and for the United States, Butman and Raymond
458 (2011) estimated 8690 g CO₂ m⁻² y⁻¹.

459 The monitoring data used for analysis is generally collected during the daytime when
460 CO₂ concentrations usually are lower due to photosynthesis compared to nighttime (Rocher-Ros
461 et al., 2020; Sand-Jensen & Frost-Christensen, 1998) which could result in the underestimation
462 of large-scale CO₂ fluxes. Multiple studies have found higher CO₂ fluxes in streams during
463 nighttime than daytime (Attermeyer et al., 2021; Gómez-Gener et al., 2021). The degree of
464 underestimation depends on the productivity of benthic primary producers and could thus be
465 substantial in a Danish setting (Alnoee et al., 2020; Kelly et al., 1983; Sand-Jensen et al., 2022a).
466 Diurnal measurements from multiple sites in River Odense show that fluxes are significantly
467 higher during the night than day and that the differences were most pronounced in spring and
468 summer, i.e. 38 and 17% higher, respectively (Weimann et al., 2024).

469 Another essential parameter for upscaling fluxes is the stream area (Wallin et al., 2018).
470 In our approach, we apply empirical relationships between upstream area and stream width,
471 which does not consider seasonal variations. The smallest streams are not part of the stream
472 network included in the DK-model. Our stream network correspond to approximately 29.5 % of
473 the length and 75% of the area compared to previously published data on stream length and area
474 for Denmark (Sand-Jensen et al., 2006). As smaller streams often have higher CO₂
475 concentrations and dominate the flux (Butman & Raymond, 2011; Wallin et al., 2018), the
476 resulting large-scale estimates are underestimated. The increasing availability of high-resolution
477 remote sensing imagery should enable improved stream area inventories in the future. While this
478 can be challenging in certain habitats such as forests, better mapping is needed, particularly
479 during the cold wet seasons when emissions are higher. Meanwhile, upscaling relies on empirical
480 relationships as a function of the catchment area or discharge (Liu et al., 2022), which preferably
481 should originate from the study region.

482 Driven by climate change, precipitation has increased (Pasten-Zapata et al., 2019)
483 yielding higher groundwater levels in Denmark during the last decades bringing groundwater
484 closer to the terrain and increasing the extent of flooding low-lying terrain (Seidenfaden et al.,
485 2022). This development is expected to continue in the future, elevating the nationally averaged
486 groundwater table by 0.12 m towards the end of the century (Seidenfaden et al., 2022).
487 Individual climate models do however predict an average change of over 0.4 m with large spatial
488 variations. This change is expected to increase the CO₂ flux from streams due to a greater influx
489 of CO₂-rich groundwater and release from wider streams and periodically inundated terrestrial
490 areas with easily degradable organic matter.

491 5 Conclusions

492 This study highlights the utility of machine learning models in predicting stream CO₂
493 concentrations and in turn estimating fluxes in Denmark. The final Random Forest model
494 appeared to perform well, albeit with overestimation at lower concentration levels but captured
495 the expected seasonal patterns in the stream network. The most important predictors were
496 catchment characteristics related to soil-groundwater-stream connectivity and seasonal
497 variations. An apparent validation exercise using instantaneous *in-situ* CO₂ flux measurements
498 suggests future research efforts should aim at refining models at local scales and improve
499 estimation of gas transfer velocity at larger scales. The study demonstrates the potential for
500 predicting large-scale patterns in environmental variables such as CO₂ fluxes by integrating
501 hydrological models and machine learning techniques. These findings have implications not only
502 for ecosystem modeling but also for informing management strategies to adapt to stream carbon
503 dynamics in a changing climate.

504 Acknowledgements

505 This work was supported by a grant to Kaj Sand-Jensen from the Independent Research
506 Fund Denmark (0217-00112B). We thank the two anonymous reviewers for their valuable
507 comments, which improved the manuscript.

508 Data availability statement

509 Data used for the analysis are available from the sources cited in the main text. The DK-
510 model data can be downloaded from <https://hipdata.dk/>. The flow components are available upon
511 request, since they are not available via the data portal. The measurements of stream CO₂ fluxes,
512 predicted CO₂ concentrations, estimated CO₂ fluxes, and scripts used for the analysis and figures
513 are available from an online repository (<https://doi.org/10.5281/zenodo.11072444>; Martinsen et
514 al., 2024).

515 Author contributions

516 Conceptualization: KTM, JK, KSJ
517 Data curation: KTM, JK, VB, JEK, TS
518 Formal Analysis: KTM, JK, KSJ
519 Funding acquisition: KSJ
520 Investigation: KTM, VB, TS, JEK
521 Methodology: KTM, JK
522 Writing – original draft: KTM, KSJ, JK
523 Writing – review & editing: KTM, KSJ, VB, TS, JEK, JK

524 References

525 Abril, G., Bouillon, S., Darchambeau, F., Teodoru, C. R., Marwick, T. R., Tamoooh, F., et al. (2015).
526 Technical Note: Large overestimation of pCO₂ calculated from pH and alkalinity in acidic,
527 organic-rich freshwaters. *Biogeosciences*, 12(1), 67–78. <https://doi.org/10.5194/bg-12-67-2015>

- 528 Adhikari, K., Kheir, R. B., Greve, M. B., Bøcher, P. K., Malone, B. P., Minasny, B., et al. (2013). High-
529 Resolution 3-D Mapping of Soil Texture in Denmark. *Soil Science Society of America Journal*,
530 77(3), 860–876. <https://doi.org/10.2136/sssaj2012.0275>
- 531 Alnoee, A. B., Riis, T., & Baattrup-Pedersen, A. (2016). Comparison of metabolic rates among
532 macrophyte and nonmacrophyte habitats in streams. *Freshwater Science*, 35(3), 834–844.
533 <https://doi.org/10.1086/687842>
- 534 Alnoee, A. B., Levi, P. S., Baattrup-Pedersen, A., & Riis, T. (2020). Macrophytes enhance reach-scale
535 metabolism on a daily, seasonal and annual basis in agricultural lowland streams. *Aquatic
536 Sciences*, 83(1), 11. <https://doi.org/10.1007/s00027-020-00766-4>
- 537 Attermeyer, K., Casas-Ruiz, J. P., Fuss, T., Pastor, A., Cauvy-Fraunié, S., Sheath, D., et al. (2021).
538 Carbon dioxide fluxes increase from day to night across European streams. *Communications
539 Earth & Environment*, 2(1), 1–8. <https://doi.org/10.1038/s43247-021-00192-w>
- 540 Bastviken, D., Sundgren, I., Natchimuthu, S., Reyier, H., & Gålfalk, M. (2015). Technical Note: Cost-
541 efficient approaches to measure carbon dioxide (CO₂) fluxes and concentrations in terrestrial and
542 aquatic environments using mini loggers. *Biogeosciences*, 12(12), 3849–3859.
543 <https://doi.org/10.5194/bg-12-3849-2015>
- 544 Beaulieu, J. J., Shuster, W. D., & Rebholz, J. A. (2012). Controls on gas transfer velocities in a large
545 river. *Journal of Geophysical Research: Biogeosciences*, 117(G2).
546 <https://doi.org/10.1029/2011JG001794>
- 547 Breiman, L. (2001). Statistical modeling: The two cultures (with comments and a rejoinder by the author).
548 *Statistical Science*, 16(3), 199–231. <https://doi.org/10.1214/ss/1009213726>
- 549 Butman, D., & Raymond, P. A. (2011). Significant efflux of carbon dioxide from streams and rivers in
550 the United States. *Nature Geoscience*, 4(12), 839–842. <https://doi.org/10.1038/ngeo1294>
- 551 Butman, D., Stackpoole, S., Stets, E., McDonald, C. P., Clow, D. W., & Striegl, R. G. (2016). Aquatic
552 carbon cycling in the conterminous United States and implications for terrestrial carbon
553 accounting. *Proceedings of the National Academy of Sciences*, 113(1), 58–63.
- 554 Cole, J. J., Prairie, Y. T., Caraco, N. F., McDowell, W. H., Tranvik, L. J., Striegl, R. G., et al. (2007).
555 Plumbing the global carbon cycle: Integrating inland waters into the terrestrial carbon budget.
556 *Ecosystems*, 10(1), 172–185. <https://doi.org/10.1007/s10021-006-9013-8>
- 557 Crawford, J. T., Lottig, N. R., Stanley, E. H., Walker, J. F., Hanson, P. C., Finlay, J. C., & Striegl, R. G.
558 (2014). CO₂ and CH₄ emissions from streams in a lake-rich landscape: Patterns, controls, and
559 regional significance. *Global Biogeochemical Cycles*, 28(3), 197–210.
560 <https://doi.org/10.1002/2013GB004661>
- 561 Demars, B. O., & Trémolières, M. (2009). Aquatic macrophytes as bioindicators of carbon dioxide in
562 groundwater fed rivers. *Science of the Total Environment*, 407(16), 4752–4763.
563 <https://doi.org/10.1016/j.scitotenv.2009.04.017>
- 564 Duvert, C., Butman, D. E., Marx, A., Ribolzi, O., & Hutley, L. B. (2018). CO₂ evasion along streams
565 driven by groundwater inputs and geomorphic controls. *Nature Geoscience*, 11(11), 813–818.
566 <https://doi.org/10.1038/s41561-018-0245-y>
- 567 Gómez-Gener, L., Rocher-Ros, G., Battin, T., Cohen, M. J., Dalmagro, H. J., Dinsmore, K. J., et al.
568 (2021). Global carbon dioxide efflux from rivers enhanced by high nocturnal emissions. *Nature
569 Geoscience*, 14(5), 289–294. <https://doi.org/10.1038/s41561-021-00722-3>
- 570 Gran, G. (1952). Determination of the equivalence point in potentiometric titrations. Part II. *Analyst*,
571 77(920), 661–671. <https://doi.org/10.1039/an9527700661>

- 572 Halbedel, S., & Koschorreck, M. (2013). Regulation of CO₂ emissions from temperate streams and
573 reservoirs. *Biogeosciences*, 10(11), 7539–7551.
- 574 Hastie, A., Lauerwald, R., Weyhenmeyer, G., Sobek, S., Verpoorter, C., & Regnier, P. (2018). CO₂
575 evasion from boreal lakes: Revised estimate, drivers of spatial variability, and future projections.
576 *Global Change Biology*, 24(2), 711–728.
- 577 Henriksen, H. J., Schneider, R., Koch, J., Ondracek, M., Troldborg, L., Seidenfaden, I. K., et al. (2023). A
578 New Digital Twin for Climate Change Adaptation, Water Management, and Disaster Risk
579 Reduction (HIP Digital Twin). *Water*, 15(1), 25. <https://doi.org/10.3390/w15010025>
- 580 Hofmann, A. F., Soetaert, K., Middelburg, J. J., & Meysman, F. J. R. (2010). AquaEnv - An Aquatic
581 Acid-Base Modelling Environment in R. *Aquatic Geochemistry*, 16, 507–546.
582 <https://doi.org/10.1007/s10498-009-9084-1>
- 583 Højberg, A. L., Troldborg, L., Stisen, S., Christensen, B. B. S., & Henriksen, H. J. (2013). Stakeholder
584 driven update and improvement of a national water resources model. *Environmental Modelling &*
585 *Software*, 40, 202–213. <https://doi.org/10.1016/j.envsoft.2012.09.010>
- 586 Hotchkiss, E. R., Hall Jr, R. O., Sponseller, R. A., Butman, D., Klaminder, J., Laudon, H., et al. (2015).
587 Sources of and processes controlling CO₂ emissions change with the size of streams and rivers.
588 *Nature Geoscience*, 8(9), 696. <https://doi.org/10.1038/ngeo2507>
- 589 Humborg, C., Mörth, C.-M., Sundbom, M., Borg, H., Blenckner, T., Giesler, R., & Ittekkot, V. (2010).
590 CO₂ supersaturation along the aquatic conduit in Swedish watersheds as constrained by terrestrial
591 respiration, aquatic respiration and weathering. *Global Change Biology*, 16(7), 1966–1978.
592 <https://doi.org/10.1111/j.1365-2486.2009.02092.x>
- 593 Hutchins, R. H. S., Prairie, Y. T., & Giorgio, P. A. del. (2019). Large-Scale Landscape Drivers of CO₂,
594 CH₄, DOC, and DIC in Boreal River Networks. *Global Biogeochemical Cycles*, 33(2), 125–142.
595 <https://doi.org/10.1029/2018GB006106>
- 596 Jähne, B., Heinz, G., & Dietrich, W. (1987). Measurement of the diffusion coefficients of sparingly
597 soluble gases in water. *J Geophys Res*, 92(C10), 10767–10776.
598 <https://doi.org/10.1029/jc092ic10p10767>
- 599 James, G., Witten, D., Hastie, T., & Tibshirani, R. (2013). *An Introduction to Statistical Learning* (Vol.
600 103). New York: Springer. <https://doi.org/10.1007/978-1-4614-7138-7>
- 601 Jones, J. B., & Mulholland, P. J. (1998). Influence of drainage basin topography and elevation on carbon
602 dioxide and methane supersaturation of stream water. *Biogeochemistry*, 40(1), 57–72.
603 <https://doi.org/10.1023/A:1005914121280>
- 604 Kelly, M. G., Thyssen, N., & Moeslund, B. (1983). Light and the annual variation of oxygen- and carbon-
605 based measurements of productivity in a macrophyte-dominated river1. *Limnology and*
606 *Oceanography*, 28(3), 503–515. <https://doi.org/10.4319/lo.1983.28.3.0503>
- 607 Koch, J., Gotfredsen, J., Schneider, R., Troldborg, L., Stisen, S., & Henriksen, H. J. (2021). High
608 Resolution Water Table Modeling of the Shallow Groundwater Using a Knowledge-Guided
609 Gradient Boosting Decision Tree Model. *Frontiers in Water*, 3, 701726.
- 610 Lauerwald, R., Laruelle, G. G., Hartmann, J., Ciais, P., & Regnier, P. A. G. (2015). Spatial patterns in
611 CO₂ evasion from the global river network. *Global Biogeochemical Cycles*, 29(5), 534–554.
612 <https://doi.org/10.1002/2014gb004941>
- 613 Lauridsen, T. L., Søndergaard, M., Jensen, J. P., & Jeppesen, E. (2005). *Investigations in lakes (in danish)*
614 (p. 234). Danish Center for Environment. Retrieved from <https://odaforalle.au.dk/>

- 615 Levin, G. (2022). *Basemap04. Documentation of the data and method for elaboration of a land use and*
616 *land cover map for Denmark*. DCE – Danish Centre for Environment and Energy: Aarhus
617 University. Retrieved from <http://dce2.au.dk/pub/TR252.pdf>
- 618 Lindsay, J. B. (2016). Whitebox GAT: A case study in geomorphometric analysis. *Computers &*
619 *Geosciences*, 95, 75–84. <https://doi.org/10.1016/j.cageo.2016.07.003>
- 620 Lindsay, J. B. (2016). Efficient hybrid breaching-filling sink removal methods for flow path enforcement
621 in digital elevation models. *Hydrological Processes*, 30(6), 846–857.
622 <https://doi.org/10.1002/hyp.10648>
- 623 Liu, S., & Raymond, P. A. (2018). Hydrologic controls on pCO₂ and CO₂ efflux in US streams and rivers.
624 *Limnology and Oceanography Letters*, 3(6), 428–435.
- 625 Liu, S., Kuhn, C., Amatulli, G., Aho, K., Butman, D. E., Allen, G. H., et al. (2022). The importance of
626 hydrology in routing terrestrial carbon to the atmosphere via global streams and rivers.
627 *Proceedings of the National Academy of Sciences*, 119(11), e2106322119.
628 <https://doi.org/10.1073/pnas.2106322119>
- 629 Long, H., Vihermaa, L., Waldron, S., Hoey, T., Quemin, S., & Newton, J. (2015). Hydraulics are a first-
630 order control on CO₂ efflux from fluvial systems. *Journal of Geophysical Research: Biogeosciences*, 120(10), 1912–1922. <https://doi.org/10.1002/2015JG002955>
- 632 Lupon, A., Denfeld, B. A., Laudon, H., Leach, J., Karlsson, J., & Sponseller, R. A. (2019). Groundwater
633 inflows control patterns and sources of greenhouse gas emissions from streams. *Limnology and*
634 *Oceanography*, 64(4), 1545–1557. <https://doi.org/10.1002/lno.11134>
- 635 Martinsen, K. T., Kragh, T., & Sand-Jensen, K. (2020). Carbon dioxide partial pressure and emission
636 throughout the Scandinavian stream network. *Global Biogeochemical Cycles*, 34(12),
637 e2020GB006703. <https://doi.org/10.1029/2020GB006703>
- 638 Martinsen, K. T., Sand-Jensen, K., Bergmann, V., Skjærlund, T., Kjær, J. E., & Koch, J. (2024). Seasonal
639 carbon dioxide concentrations and fluxes throughout Denmark's stream network [Dataset].
640 Zenodo. <https://doi.org/10.5281/zenodo.11072444>
- 641 Marx, A., Dusek, J., Jankovec, J., Sanda, M., Vogel, T., van Geldern, R., et al. (2017). A review of CO₂
642 and associated carbon dynamics in headwater streams: A global perspective. *Reviews of*
643 *Geophysics*, 55(2), 560–585. <https://doi.org/10.1002/2016rg000547>
- 644 O'Callaghan, J. F., & Mark, D. M. (1984). The extraction of drainage networks from digital elevation
645 data. *Computer Vision, Graphics, and Image Processing*, 28(3), 323–344.
646 [https://doi.org/10.1016/S0734-189X\(84\)80011-0](https://doi.org/10.1016/S0734-189X(84)80011-0)
- 647 Olden, J. D., Lawler, J. J., & Poff, N. L. (2008). Machine learning methods without tears: A primer for
648 ecologists. *The Quarterly Review of Biology*, 83(2), 171–193. <https://doi.org/10.1086/587826>
- 649 Olsen, M., & Højberg, A. L. (2011). *Expansion of stream network (in Danish)*. Copenhagen: Geological
650 Survey of Denmark and Greenland (GEUS).
- 651 Pasten-Zapata, E., Sonnenborg, T. O., & Refsgaard, J. C. (2019). Climate change: Sources of uncertainty
652 in precipitation and temperature projections for Denmark. *GEUS Bulletin*, 43.
653 <https://doi.org/10.34194/GEUSB-201943-01-02>
- 654 Pedregosa, F., Varoquaux, G., Gramfort, A., Michel, V., Thirion, B., Grisel, O., et al. (2011). Scikit-learn:
655 Machine learning in Python. *The Journal of Machine Learning Research*, 12, 2825–2830.
- 656 Raymond, P. A., Zappa, C. J., Butman, D., Bott, T. L., Potter, J., Mulholland, P., et al. (2012). Scaling the
657 gas transfer velocity and hydraulic geometry in streams and small rivers. *Limnology and*

- 658 *Oceanography: Fluids and Environments*, 2(1), 41–53. <https://doi.org/10.1215/21573689-1597669>
- 660 Raymond, P. A., Hartmann, J., Lauerwald, R., Sobek, S., McDonald, C., Hoover, M., et al. (2013). Global
661 carbon dioxide emissions from inland waters. *Nature*, 503(7476), 355–359.
662 <https://doi.org/10.1038/nature12760>
- 663 Rebsdorf, A., Thyssen, N., & Erlandsen, M. (1991). Regional and temporal variation in pH, alkalinity and
664 carbon dioxide in Danish streams, related to soil type and land use. *Freshwater Biology*, 25(3),
665 419–435. <https://doi.org/10.1111/j.1365-2427.1991.tb01386.x>
- 666 Rennó, C. D., Nobre, A. D., Cuartas, L. A., Soares, J. V., Hodnett, M. G., Tomasella, J., & Waterloo, M.
667 J. (2008). HAND, a new terrain descriptor using SRTM-DEM: Mapping terra-firme rainforest
668 environments in Amazonia. *Remote Sensing of Environment*, 112(9), 3469–3481.
669 <https://doi.org/10.1016/j.rse.2008.03.018>
- 670 Rocher-Ros, G., Sponseller, R. A., Lidberg, W., Mört, C.-M., & Giesler, R. (2019). Landscape process
671 domains drive patterns of CO₂ evasion from river networks. *Limnology and Oceanography
672 Letters*, 4(4), 87–95. <https://doi.org/10.1002/lo2.10108>
- 673 Rocher-Ros, G., Sponseller, R. A., Bergström, A.-K., Myrstener, M., & Giesler, R. (2020). Stream
674 metabolism controls diel patterns and evasion of CO₂ in Arctic streams. *Global Change Biology*,
675 26(3), 1400–1413. <https://doi.org/10.1111/gcb.14895>
- 676 Salter, M. E., Upstill-Goddard, R. C., Nightingale, P. D., Archer, S. D., Blomquist, B., Ho, D. T., et al.
677 (2011). Impact of an artificial surfactant release on air-sea gas fluxes during Deep Ocean Gas
678 Exchange Experiment II. *Journal of Geophysical Research: Oceans*, 116(C11).
679 <https://doi.org/10.1029/2011JC007023>
- 680 Sand-Jensen, K., Friberg, N., & Murphy, J. (Eds.). (2006). *Running Waters: Historical development and
681 restoration of lowland Danish streams*. Aarhus Universitetsforlag, Denmark.
- 682 Sand-Jensen, K. (2008). Drag forces on common plant species in temperate streams: Consequences of
683 morphology, velocity and biomass. *Hydrobiologia*, 610(1), 307–319.
684 <https://doi.org/10.1007/s10750-008-9446-5>
- 685 Sand-Jensen, K., & Frost-Christensen, H. (1998). Photosynthesis of amphibious and obligately
686 submerged plants in CO₂-rich lowland streams. *Oecologia*, 117(1–2), 31–39.
687 <https://doi.org/10.1007/s004420050628>
- 688 Sand-Jensen, K., & Mebus, J. R. (1996). Fine-Scale Patterns of Water Velocity within Macrophyte
689 Patches in Streams. *Oikos*, 76(1), 169–180. <https://doi.org/10.2307/3545759>
- 690 Sand-Jensen, K., & Staehr, P. A. (2012). CO₂ dynamics along Danish lowland streams: Water-air
691 gradients, piston velocities and evasion rates. *Biogeochemistry*, 111(1–3), 615–628.
692 <https://doi.org/10.1007/s10533-011-9696-6>
- 693 Sand-Jensen, K., Riis, T., Kjær, J. E., & Martinsen, K. T. (2022a). Stream-Lake Connectivity Is an
694 Important Control of Fluvial CO₂ Concentrations and Emissions in Catchments. *Earth and Space
695 Science*, 9(12), e2022EA002664. <https://doi.org/10.1029/2022EA002664>
- 696 Sand-Jensen, K., Riis, T., & Martinsen, K. T. (2022b). Photosynthesis, growth, and distribution of plants
697 in lowland streams—A synthesis and new data analyses of 40 years research. *Freshwater
698 Biology*, 67(7), 1255–1271. <https://doi.org/10.1111/fwb.13915>
- 699 Scharling, M. (1999a). *Climate grid Denmark: precipitation 10*10 km (ver. 2) (in Danish)* (Vol. 99).
700 Danish Meteorological Institute.

- 701 Scharling, M. (1999b). *Climate grid Denmark: precipitation, air temperature, and potential*
702 *evapotranspiration 20x20 & 40x40 km: method description (in Danish)*. Danish Meteorological
703 Institute.
- 704 SDFI. (2021). Agency for Datasupply and Infrastructure, SDFI. Accessed October 2021.
705 Retrieved from <https://dataforsyningen.dk/data>
- 706 Seidenfaden, I. K., Sonnenborg, T. O., Stisen, S., & Kidmose, J. (2022). Quantification of climate change
707 sensitivity of shallow and deep groundwater in Denmark. *Journal of Hydrology: Regional*
708 *Studies*, 41, 101100. <https://doi.org/10.1016/j.ejrh.2022.101100>
- 709 Smits, A. P., Schindler, D. E., Holtgrieve, G. W., Jankowski, K. J., & French, D. W. (2017). Watershed
710 geomorphology interacts with precipitation to influence the magnitude and source of CO₂
711 emissions from Alaskan streams. *Journal of Geophysical Research: Biogeosciences*, 122(8),
712 1903–1921. <https://doi.org/10.1002/2017jg003792>
- 713 Soltani, M., Bjerre, E., Koch, J., & Stisen, S. (2021). Integrating remote sensing data in optimization of a
714 national water resources model to improve the spatial pattern performance of evapotranspiration.
715 *Journal of Hydrology*, 603, 127026. <https://doi.org/10.1016/j.jhydrol.2021.127026>
- 716 Tarboton, D. G. (2017). Terrain analysis using digital elevation models (TauDEM) Utah Water
717 Research Laboratory, Utah State University. Retrieved from
718 <http://hydrology.usu.edu/taudem/taudem5/index.html>
- 719 Thyssen, N., & Erlandsen, M. (1987). Reaeration of Oxygen in Shallow, Macrophyte Rich Streams: II.
720 Relationship between the Reaeration Rate Coefficient and Hydraulic Properties. *Internationale*
721 *Revue Der Gesamten Hydrobiologie Und Hydrographie*, 72(5), 575–597.
722 <https://doi.org/10.1002/iroh.19870720505>
- 723 Ulseth, A. J., Hall, R. O., Boix Canadell, M., Madinger, H. L., Niayifar, A., & Battin, T. J. (2019).
724 Distinct air–water gas exchange regimes in low- and high-energy streams. *Nature Geoscience*,
725 12(4), 259–263. <https://doi.org/10.1038/s41561-019-0324-8>
- 726 Wallin, M. B., Öquist, M. G., Buffam, I., Billett, M. F., Nisell, J., & Bishop, K. H. (2011). Spatiotemporal
727 variability of the gas transfer coefficient (KCO₂) in boreal streams: Implications for large scale
728 estimates of CO₂ evasion. *Global Biogeochemical Cycles*, 25(3).
729 <https://doi.org/10.1029/2010gb003975>
- 730 Wallin, M. B., Grabs, T., Buffam, I., Laudon, H., Ågren, A., Öquist, M. G., & Bishop, K. (2013). Evasion
731 of CO₂ from streams—The dominant component of the carbon export through the aquatic conduit
732 in a boreal landscape. *Global Change Biology*, 19(3), 785–797. <https://doi.org/10.1111/gcb.12083>
- 733 Wallin, M. B., Campeau, A., Audet, J., Bastviken, D., Bishop, K., Kokic, J., et al. (2018). Carbon dioxide
734 and methane emissions of Swedish low-order streams - A national estimate and lessons learnt
735 from more than a decade of observations. *Limnology and Oceanography Letters*.
736 <https://doi.org/10.1002/lol2.10061>
- 737 Wang, J., Bombardelli, F. A., & Dong, X. (2021). Physically Based Scaling Models to Predict Gas
738 Transfer Velocity in Streams and Rivers. *Water Resources Research*, 57(3), e2020WR028757.
739 <https://doi.org/10.1029/2020WR028757>
- 740 Wanninkhof, R. (1992). Relationship between wind speed and gas exchange over the ocean. *J Geophys*
741 *Res-Oceans*, 97(C5), 7373–7382. <https://doi.org/10.1029/92jc00188>
- 742 Weimann, B., Kragh, T., Sø, J. S., & Sand-Jensen, K. (2024). Methane and carbon dioxide stream fluxes
743 at hourly and seasonal scales among forested and agricultural sites in a lowland Danish stream.
744 (*Submitted Manuscript*).

- 745 Weyhenmeyer, G. A., Kortelainen, P., Sobek, S., Müller, R., & Rantakari, M. (2012). Carbon dioxide in
746 boreal surface waters: A comparison of lakes and streams. *Ecosystems*, 15(8), 1295–1307.
747 <https://doi.org/10.1007/s10021-012-9585-4>